

Experimental Simulation and Verification of Position Servo Control of Mechanical Rodless Cylinder

Yeming ZHANG, Kaimin LI, Hongwei YUE, Shuangyang HE, Dongyuan LI, Kun LYU, Feng WEI

School of Mechanical and Power Engineering, Henan Polytechnic University, Jiaozuo, China

*Corresponding Author: Yeming ZHANG, E-mail: tazhangyeming@163.com

Abstract:

In order to improve the position control accuracy of rodless cylinder, the valve control cylinder system based on pneumatic proportional servo is studied deeply. According to the working principle of the mechanical rodless cylinder control system, under the condition of uniform speed, the driving voltage of the proportional valve is changed to measure multiple sets of friction force and corresponding velocity data. Analyzed the physical structure of each component in pneumatic system, established the mathematical model of pneumatic system, and introduced MATLAB system identification toolbox to identify the parameters of the transfer function. and the experiment verifies its correctness.

Keywords: mechanical rodless cylinder; friction characteristics; mathematical model; parameter identification

1 Introduction

Pneumatic technology is the technology that uses compressed air as a working medium for energy and signal transmission. It is an important means to improve production efficiency and realize automation of production process in modern industry [1-3]. With the continuous progress and development of science and technology and industrial engineering, the requirements of precision operation in industrial occasions are becoming higher and higher, and the precise control of pneumatic technology is put forward higher requirements. In order to realize the accurate control of pneumatic system, it is necessary to analyze the system comprehensively. In the pneumatic valve control cylinder system, the linear model can control the mass flow equation of the valve according to the proportional direction, the mass flow continuity equation of the cylinder, and the dynamics of the cylinder. equation linearization treatment obtained [4-6].

The Pedro Luis Andrighetto^[7] Lee E.Schroeder^[8], Brazil in the United States and the laboratory of Beijing Institute of Technology^[9] used the test scheme of driving the load cylinder motion directly with compressed air. Zhang Baihai of Beijing Institute of Technology^[10] studied the effect of temperature on cylinder friction force, and its experimental results show that the maximum static friction force, viscosity the friction coefficient decreases with the increase of temperature, while the coulomb friction force is

less affected by temperature. On the basis of experiments, T. Raparelli and G. Belfore et al. of Italy used the finite element method to analyze the friction force. Through the simulation of the force and deformation of the sealing ring and the verification of the experimental results, the changes of the force and friction force of the double O seal ring and the lip seal ring under different lubrication and working pressure conditions were studied^[11-14].

Liu Xiangming et al.^[15] of Wuhan University of Engineering identified the third order electro-hydraulic servo system model by using the M sequence of DAQ acquisition assistant as the excitation signal of the system in LabView environment. song tao et al.^[16] of nanjing university of technology established a symmetrical cylinder hydraulic system model. the input and output data of the controlled object of the system were simulated in the MATLAB. the identification model of least square method was used to identify the system, which provided a more accurate system model for further research. Kong Xiangzhen^[17] of Shandong University adopted the optimal design problem in the identification process, A pseudo random sequence similar to white noise is used as input signal to continuously excite the controlled object, and the whole system is identified. The input and output experimental data are identified by MATLAB the system identification toolbox. Finally, the transfer function of the whole closed-loop system is obtained. In industrial control, the theory of system identification has been developed

for decades, and the research and application are more and more extensive, but the research and application in pneumatic servo control need to be further excavated.

Based on the friction experiment, the Stribeck friction model of the rodless cylinder is established. The mass flow equation of proportional valve, the mass flow equation of cylinder and the dynamic equation are established and linearized in the middle position of cylinder. Based on the experimental test, the input and output data of valve control cylinder are obtained, and the parameters of the transfer function obtained are identified in the MATLAB system identification toolbox.

2 Construction of Control System

The working principle of pneumatic servo position control system with mechanical rodless cylinder as control object is shown in figure 1. The industrial control computer sends out the target displacement instruction, which converts the numerical signal to the analog voltage signal of 0-10 V through the D/A conversion module, and the analog voltage signal controls the valve opening in the proportional direction. A measuring system detects the

displacement of the rodless cylinder in real time and transmits the displacement signal to the data acquisition card of the industrial control computer in the form of TTL level. The air compressor produces compressed air as a source of fluid power, and flows through pneumatic triplets (air filters, pressure relief valves, oil mist) to transmit clean compressed air into proportional control valves Inside. By using the feedback deviation control, the IPC processes the feedback detection signal and the deviation value of the target value of the displacement measurement system according to the software platform LabVIEW as the upper computer to adjust the valve opening size of the proportional direction control valve in real time, and then reduce the displacement deviation of the rodless cylinder, so that the movement of the rodless cylinder finally reaches the ideal target position. Through the above principle, the pneumatic proportional servo control system can control the precise position of the mechanical rodless cylinder.

According to the experimental principle, set up the following physical experimental platform, as shown in figure 2.

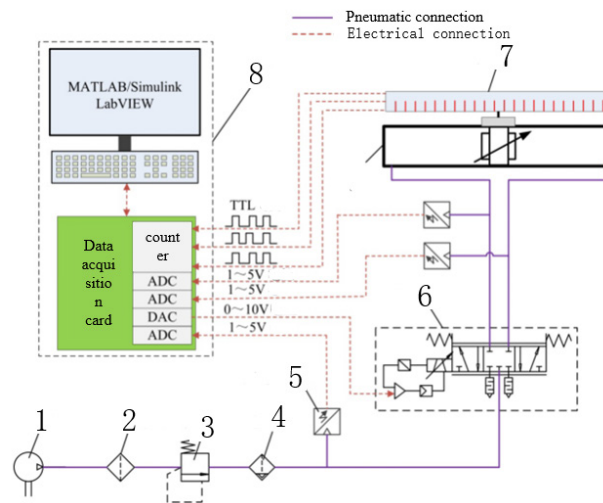


Figure 1 Schematic diagram of pneumatic servo position control system

(1-air compressor; 2-air filter; 3-air regulator; 4-air lubricator; 5-pressure transmitter; 6-proportional directional control valve; 7-Rodless cylinder; 8-IPC).

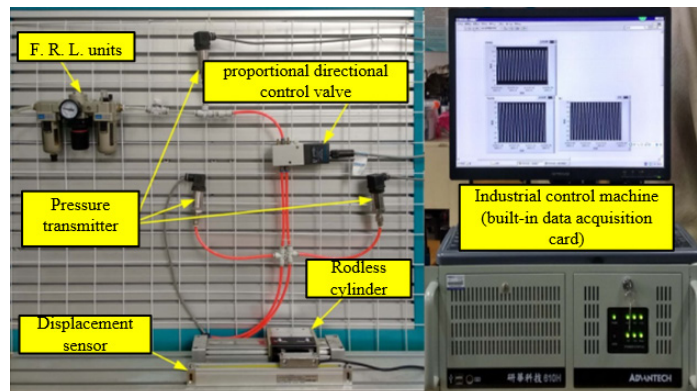


Figure 2 Experimental Platform of Servo Position Control System

This system proportional direction control valve selects the three-bit five-way proportional direction control valve produced by Germany FESTO Company as the control element, the power supply is DC 24 V, the pressure use range is 0~1 MPa, take the mechanical rodless cylinder as the end pneumatic actuator of the system. In order to ensure the accuracy of measurement and convenient installation, the displacement feedback element selected by this select the grating ruler line displacement sensor.

Checking the displacement characteristics of the Slide valve requires measuring the displacement of the Side valve of the proportional control valve with the change of the driving voltage. Select the HG-C1050 model laser displacement sensor produced by Panasonic Japan is a measuring element. A pressure transducer of MIK-P300 type is selected as the measuring element. The models and parameters of each component are shown in Table 1.

Table 1 Types and working parameters of system components

Components	Model	Parameter
Air compressor	Medical Silent Piston Air Compressor	Working pressure 0.4~0.7MPa
F. R. L. units	AC3000-03	Voltage regulation range 0-1MPa
proportional directional control valve	MPYE-5-M5-010-B	5-bit 3-way valve, 0-10V driving voltage
Mechanical rodless cylinder	SMC MYC25G-110L	Travel itinerary 110mm, Pressure range 0.1-0.8MPa
Grating Displacement Sensor	JCXE-DC	Operating voltage 5V, Travel itinerary 200mm
Laser displacement sensor	Panasonic HG-C1050	Scope of measurement ± 15 mm, Precision 30 μ m
Pressure transmitter	MIK-P300	Range 0-1.0MPa, Precision 0.3%F.S.
Flow sensor	SFAB-200U-HQ8-2SV-M12	Range 0-200L/min, Voltage voltage 24V

3 Friction characteristics of rodless cylinder

3.1 Measurement method of friction parameters

In the servo system, the friction force always exists in the whole motion process. Compared with the driving force of compressed air, the friction force of pneumatic end actuator is relatively large, and the friction force presents nonlinearly in motion, which seriously affects the accurate positioning of cylinder position. The friction of the cylinder mainly exists in the friction between the piston and the inner wall of the cylinder, between the piston and the inner sealing belt, and between the sliding block and the external dust-proof sealing belt. When the rodless cylinder moves in a straight line at a constant speed, the acceleration is zero, and the driving force only works against friction. According to Newton's first law of motion, its mathematical expression is as follows:

$$F_f = A_a p_a - A_b p_b \quad (1)$$

Therefore, when the cylinder speed is constant, the pressure difference between the two chambers is the friction value to be measured. Under the condition of constant supply gas pressure, by changing the driving voltage of proportional valve to change the opening of valve port, the movement speed of piston will also change. In the experiment, the friction force at different speeds was measured, and the friction-velocity curve was obtained. In the Stribeck friction model, there is the maximum static friction force F_s , Coulomb friction F_c , Critical Stribeck velocity \dot{y}_s And viscous friction coefficient σ A total of four parameters need to be measured [53]. The measurement method is as follows:

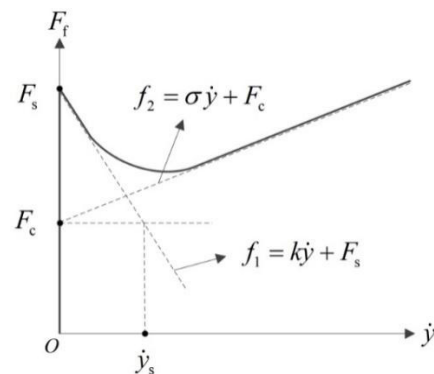


Figure 3 Stribeck friction model curve

In figure 3, in order to describe the state of friction model intuitively, auxiliary dotted lines are added. When the velocity of the piston is in the zero speed region, the total friction force is F_s . With the increase of the speed, the cylinder movement in the low speed stage can be approximately linear f_1 express. Let k is the slope of this line, and the intersection of the line and the ordinate axis is F_s . As the speed continues to increase. It is represented by a straight line σ , the slope is σ , the intersection point with the vertical axis is F_c . Cross the Coulomb friction f_2 coordinates point as the intersection point of the parallel line of the abscissa axis and the curve f_2 , and then make a vertical line to the abscissa axis, the critical Stribeck velocity is the intersection of the vertical line and the abscissa axis \dot{y}_s .

3.2 Measurement and analysis of friction parameters

When the supply gas pressure is 0.6MPa, the pressure difference between the two chambers at different constant

speeds is measured by changing the driving voltage of the proportional directional control valve. The pressure difference of each group under uniform velocity is substituted into the corresponding friction force calculated by formula (1). Figure 4 shows the pressure difference and displacement curve of the cylinder at low speed when the driving voltage is 4.91V. The maximum static friction force can be obtained by substituting the maximum pressure difference into formula (1), and the friction force at this speed can be obtained by substituting the average pressure difference in the dotted box. It can be seen from the displacement curve that there is a small displacement before the continuous sliding of the cylinder, which is often called the displacement before sliding. The measured friction velocity of each group is summed up and fitted to form a relationship curve, as shown in figure 5. The four parameter values of Stribeck friction model obtained by making auxiliary lines are shown in figure 6. The specific parameter values are shown in table 2.

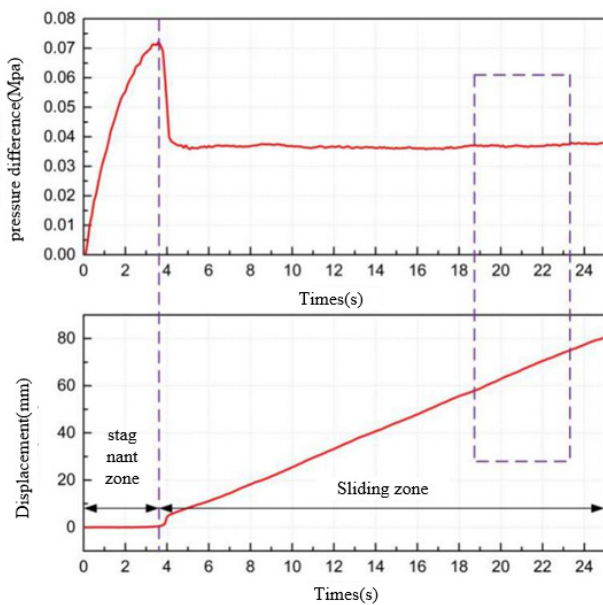


Figure 4 low speed operation process of cylinder

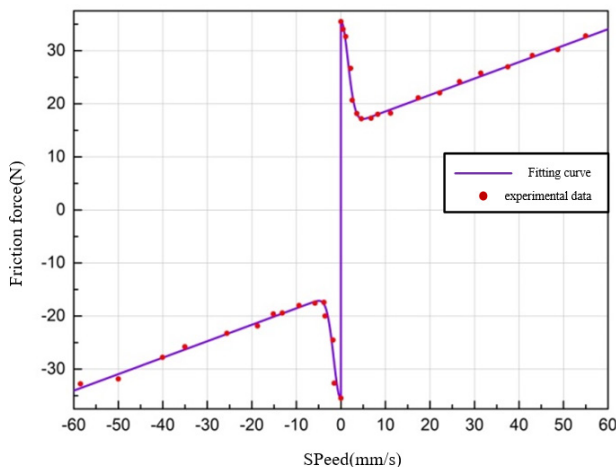


Figure 5 friction curve fitting

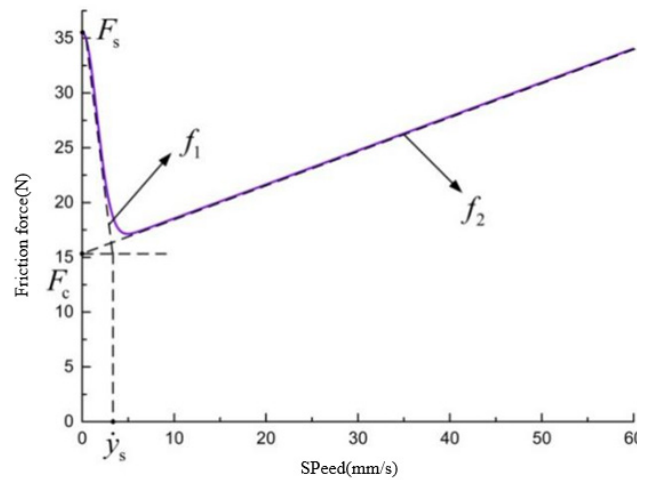


Figure 6 Friction parameter diagram

Table 2 Stribeck friction parameter values

Parameters	Value
F_s	35.48 (N)
F_c	15.31 (N)
\dot{y}_s	3.27 (mm/s)
σ	0.31 (N.s / mm)

4 Establishment of system model and parameter identification

4.1 Establishment of system model

By analyzing the physical structure and working principle of proportional directional control valve and rodless cylinder, the piston of rodless cylinder is connected with the external slider of cylinder mechanically, and the displacement of piston is the displacement of slider. The basic equations of valve controlled cylinder system are linearized in the middle position, and the mass flow equation of proportional valve, mass flow continuity equation of rodless cylinder and dynamic equation of are established respectively. Figure 7 describes the flow mechanism of the proportional valve controlled cylinder system. The left chamber of the proportional valve is connected with the chamber a of the cylinder, and the right chamber of the proportional valve is connected with the chamber B of the cylinder. Therefore, any chamber in the proportional valve and the corresponding connected cylinder chamber are regarded as a control body where the gas temperature and pressure are equal everywhere. The control body where the left chamber of the cylinder is located is chamber a, and the control body where the right chamber of the gas cylinder is located is chamber B. the gas flow process in the whole valve controlled cylinder system can be seen It is the process that the gas flows through the proportional valve to charge and deflate a and B cavities. Set the proportional spool slide to move to the right as a positive direction. When the valve core of the proportional directional valve moves in the positive direction, chamber

$$\sum \dot{M}_\lambda - \sum \dot{M}_\mu = \frac{dM}{dt} = \frac{d(\rho V)}{dt} = \rho \frac{dV}{dt} + V \frac{d\rho}{dt} \quad (8)$$

The continuous equation for the mass flow of the cylinder cavities A and B is as follows:

$$\begin{cases} \dot{M}_a = \rho_a \frac{dV_a}{dt} + V_a \frac{d\rho_a}{dt} \\ \dot{M}_b = \rho_b \frac{dV_b}{dt} + V_b \frac{d\rho_b}{dt} \end{cases} \quad (9)$$

The ideal state equation $\rho = p / RT$ of gas is substituted by formula (9) to obtain:

$$\begin{cases} \dot{M}_a = \frac{1}{RT_a} \left(p_a \frac{dV_a}{dt} + V_a \frac{dp_a}{dt} - \frac{p_a V_a}{T_a} \frac{dT_a}{dt} \right) \\ \dot{M}_b = \frac{1}{RT_b} \left(p_b \frac{dV_b}{dt} + V_b \frac{dp_b}{dt} - \frac{p_b V_b}{T_b} \frac{dT_b}{dt} \right) \end{cases} \quad (10)$$

From the isentropic condition:

$$T = T_0 \left(\frac{p}{p_0} \right)^{\frac{\kappa-1}{\kappa}} \quad (11)$$

In the formula, T_0 represents the initial temperature, p_0 represents initial pressure. Formula (12) can be derived from time by formula (11):

$$\frac{dT}{dt} = \frac{\kappa-1}{\kappa} \frac{T_0}{p_0} \left(\frac{p}{p_0} \right)^{\frac{1}{\kappa}} \frac{dp}{dt} = \frac{\kappa-1}{\kappa} \frac{T_0}{p} \left(\frac{p}{p_0} \right)^{\frac{\kappa-1}{\kappa}} \frac{dp}{dt} = \frac{\kappa-1}{\kappa} \frac{T}{p} \frac{dp}{dt} \quad (12)$$

Formula (12) can be obtained by substituting it for formula (10):

$$\begin{cases} \dot{M}_a = \frac{1}{RT_a \kappa} \left(V_a \frac{dp_a}{dt} + \kappa p_a \frac{dV_a}{dt} \right) \\ \dot{M}_b = \frac{1}{RT_b \kappa} \left(V_b \frac{dp_b}{dt} + \kappa p_b \frac{dV_b}{dt} \right) \end{cases} \quad (13)$$

Because the piston position in the middle of the cylinder is representative of the dynamic characteristics^[57], assuming that the parameter of the cylinder piston at the stable working point in the middle is set to the initial value under small interference, the formula (14) can be obtained. The lower corners 0a and 0b indicate the initial state of chamber a and b, respectively, T_s for supply air temperature, V_0 is half the total cylinder volume, p_0 is the initial equilibrium pressure of the two chambers when the piston is in steady state.

$$\begin{cases} \dot{M}_a = 0 + \Delta \dot{M}_a, & \dot{M}_b = 0 + \Delta \dot{M}_b \\ p_a = p_{0a} + \Delta p_a, & p_b = p_{0b} + \Delta p_b \\ V_a = V_{0a} + \Delta V_a, & V_b = V_{0b} + \Delta V_b \\ T_a = T_{0a} + \Delta T_a, & V_b = T_{0b} + \Delta T_b \end{cases} \quad (14)$$

Initial values and have the following relationships:

$$\begin{cases} \Delta \dot{V}_a = -\Delta \dot{V}_b = A \Delta \dot{y} \\ T_{0a} = T_{0b} = T_s \\ V_{0a} = V_{0b} = V_0 \\ p_{0a} = p_{0b} = p_0 \end{cases} \quad (15)$$

Since the incremental values of each physical quantity are small relative to the initial values under small

disturbances, they can be neglected in the calculation^[58]. Therefore, the incremental expression of the continuous equation for the gas mass flow in the cylinder is as follows:

$$\begin{cases} \Delta \dot{M}_a = \frac{1}{RT_s \kappa} \left[V_0 \frac{d(\Delta p_a)}{dt} + \kappa p_0 A \Delta \dot{y} \right] \\ \Delta \dot{M}_b = \frac{1}{RT_s \kappa} \left[V_0 \frac{d(\Delta p_b)}{dt} - \kappa p_0 A \Delta \dot{y} \right] \end{cases} \quad (16)$$

Equation (16) can also be written:

$$\Delta \dot{M}_a - \Delta \dot{M}_b = \frac{1}{RT_s \kappa} \left\{ V_0 \left[\frac{d(\Delta p_a)}{dt} - \frac{d(\Delta p_b)}{dt} \right] + 2\kappa p_0 A \Delta \dot{y} \right\} \quad (17)$$

4.1.3 Dynamic equation of cylinder

In figure 7, according to Newton's second theorem, the pressure difference between the chambers a and B is the power that drives the piston movement. The dynamic equation of the cylinder is as follows:

$$A(p_a - p_b) = M_L \ddot{y} + F_L + F_f \quad (18)$$

Inside, M_L represents the mass of the piston and its moving parts, F_L is the external load force, F_f represents the total friction force in motion.

4.1.4 Block diagram and transfer function of valve controlled cylinder system

The linear model of the whole system can be composed of the mass flow equation of proportional directional control valve (7), the mass flow continuity equation of cylinder (17), and the dynamic equation of cylinder (18).

$$\begin{cases} \dot{M}_a - \dot{M}_b = 2c_1 x_v - c_2 (p_a - p_b) \\ \dot{M}_a - \dot{M}_b = \frac{1}{RT_s \kappa} \left[V_0 \left(\frac{dp_a}{dt} - \frac{dp_b}{dt} \right) + 2\kappa p_0 A \dot{y} \right] \\ A(p_a - p_b) = M_L \ddot{y} + F_L + F_f \end{cases} \quad (19)$$

Make the pressure difference $p_L = p_a - p_b$, Mass flow difference $\dot{M}_L = \dot{M}_a - \dot{M}_b$, The formula (19) is transformed by pulling:

$$\begin{cases} \dot{M}_L(s) = 2c_1 x_v(s) - c_2 p_L(s) \\ \dot{M}_L(s) = \frac{1}{RT_s \kappa} \left[V_0 s p_L(s) + 2\kappa p_0 A s y(s) \right] \\ A p_L(s) = M_L s^2 y(s) + F_L(s) + F_f(s) \end{cases} \quad (20)$$

The block diagram of valve controlled cylinder system can be obtained from formula (20), as shown in figure 10.

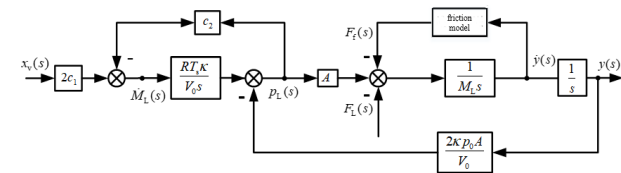


Figure 10 Block diagram of the valve-controlled cylinder system

The transfer function of the valve controlled cylinder system can be obtained by solving the simultaneous basic equations or by simplifying the block diagram.

(1) Transfer function of spool displacement x_v to cylinder output displacement y .

When $F_f=0$ and $F_L=0$, the transfer function of spool displacement x_v to output displacement y can be obtained as follows:

$$\frac{y_x(s)}{x_v(s)} = \frac{K_T \omega_n^2}{s(s^2 + 2\zeta\omega_n s + \omega_n^2)} \quad (21)$$

Among, the gain K_T is:

$$K_T = \frac{c_1 RT_s}{p_0 A} \quad (22)$$

The damping ratio ζ is:

$$\zeta = \frac{c_2 RT_s}{2A} \sqrt{\frac{\kappa M_L}{2V_0 p_0}} \quad (23)$$

The natural frequency ω_n is:

$$\omega_n = \sqrt{\frac{2\kappa p_0 A^2}{V_0 M_L}} \quad (24)$$

When $x_v=0$ and $F_L=0$, it can be obtained that the transfer function of the friction force F_f to the output displacement y is:

$$\frac{y_f(s)}{F_f(s)} = -\frac{K_T \omega_n^2}{2c_1 A} \left(\frac{V_0}{RT_s \kappa} s + c_2 \right) \frac{1}{s(s^2 + 2\zeta\omega_n s + \omega_n^2)} \quad (25)$$

In the same way, when $F_f=0$ and $F_f=0$, it can be obtained that the transfer function of friction force y to output displacement y is:

$$\frac{y_L(s)}{F_L(s)} = -\frac{K_T \omega_n^2}{2c_1 A} \left(\frac{V_0}{RT_s \kappa} s + c_2 \right) \frac{1}{s(s^2 + 2\zeta\omega_n s + \omega_n^2)} \quad (26)$$

Therefore, the total transfer function of the valve controlled cylinder system is:

$$y(s) = y_x(s) + y_f(s) + y_L(s) = \frac{K_T \omega_n^2 x_v(s) - \frac{K_T \omega_n^2 [F_f(s) + F_L(s)]}{2c_1 A} \left(\frac{V_0}{RT_s \kappa} s + c_2 \right)}{s(s^2 + 2\zeta\omega_n s + \omega_n^2)} \quad (27)$$

Because the proportional directional valve has strong linear characteristics, the transfer function can be described as follows:

$$\frac{x_v(s)}{U(s)} = K_v \quad (28)$$

In the formula, K_v represents proportional gain, U indicates the drive voltage of the valve.

The transfer function of the proportional amplifier is:

$$\frac{U(s)}{y_{in}(s) - y(s)} = K_a \quad (29)$$

In the formula, K_a represents proportional gain, y_{in} represents the input displacement.

Friction compensation is used to reduce the influence of friction on the system. According to the formulas (27), (28), (29), the block diagram of the cylinder servo system can be obtained as shown in figure 11.

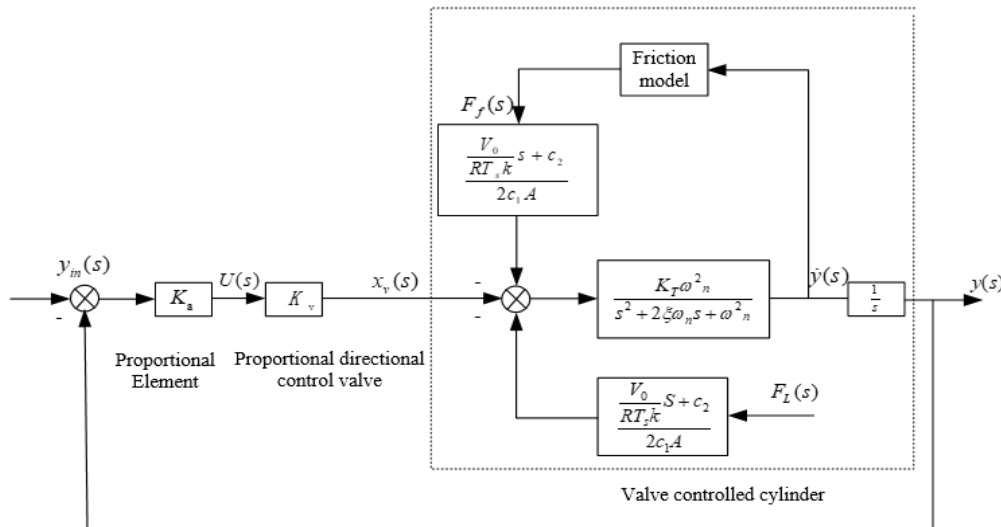


Figure 11 Block Diagram of Cylinder Position Servo System

Therefore, the open-loop transfer function of the system is:

$$H(z) = \frac{b_1 z^3 + b_2 z^2 + b_3 z + b_4}{a_1 z^3 + a_2 z^2 + a_3 z + a_4} \quad (30)$$

Formula (4-29) is discretized and its open-loop transfer function is obtained as follows:

$$H(z) = \frac{b_1 z^3 + b_2 z^2 + b_3 z + b_4}{a_1 z^3 + a_2 z^2 + a_3 z + a_4} \quad (31)$$

In the formula, b_1, b_2, b_3, b_4 and a_1, a_2, a_3, a_4 are

constant values.

4.2 Valve-controlled cylinder system identification

4.2.1 System Identification Process

System identification can be divided into open loop identification and closed loop identification. Closed-loop identification methods are divided into closed-loop direct identification and closed-loop indirect identification. The closed-loop indirect identification method is to identify the closed-loop transfer function of the whole system first,

then subtract the feedback link of the system to obtain the open-loop transfer function of the system. This method is cumbersome due to the elimination of intermediate links. Closed-loop direct identification method is to identify the open-loop transfer function of controlled object under closed-loop condition. Since the linearized system model is a third-order model and the proportional valve-controlled cylinder system has an integral part and is an open-loop unstable system, this paper uses closed-loop condition to directly identify the open-loop transfer function of the system.

M-sequence is a binary pseudo-random code sequence of approximate white noise signals as shown in figure 12. M-sequence as interference signal can fully excite the characteristics of the controlled object. The input signal is the superposition of the controller output signal and M-sequence signal, and the output signal is the cylinder displacement signal. To identify the input signal and output displacement before and after the object, the open loop system of the system is identified. Figure 13 is the identification test schematic.

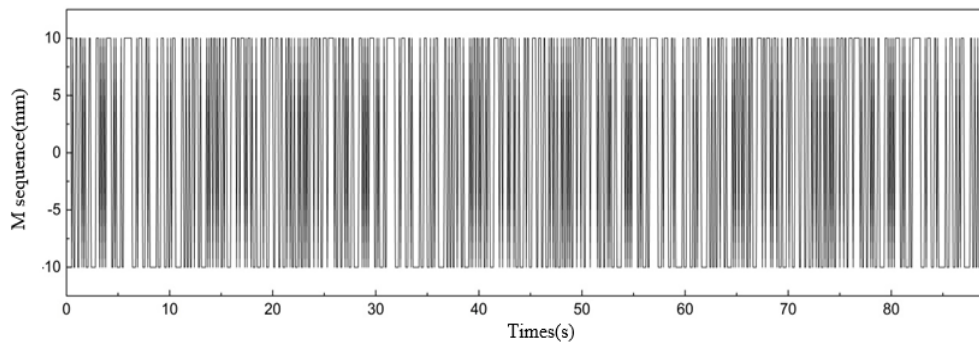


Figure 12 M-sequence signal

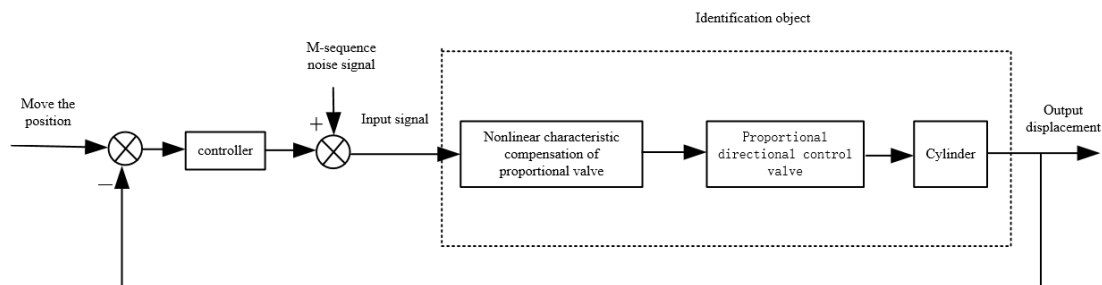


Figure 13 Identification test schematic diagram

For nonlinear systems, a parametric linearization model can be established based on the perturbation theory. During the identification process, the cylinder piston is allowed to move to the left and right, and the "near disturbance" of the input signal to the system should be in both positive and negative directions. The amplitude of input signal is not too small, it will slow down the response of the system, not fully excite the dynamic characteristics of the system and make the system identify distortion, but it should not be too large, so the input signal should be selected reasonably. Identified input and output signals are shown in figure 14.

In MATLAB, input signal and output signal are imported separately. ARX discrete transfer function model is selected for identification in time domain. The identification results are shown in figure 15.

The identified system model is:

$$H(z) = \frac{0.1496z^2 - 0.03607z + 0.1678}{z^3 - 1.4276z^2 + 0.85537z - 0.4243} \quad (32)$$

4.2.2 Experimental verification of system identification model

According to the system schematic diagram built as shown in figure 16, the input step signal and sinusoidal displacement signal are experimentally verified. Figure 17 is a comparison diagram of the results of simulation and experiment. It can be concluded that the identified system model can well reflect the dynamic characteristics of the control system.

From the previous section 4.1 (Establishment of system model) the theoretical model of the system is obtained. Under the standard input signal (step signal and sinusoidal signal), the position control of the rodless cylinder is studied experimentally, and the actual input and output data curve of the rodless cylinder is obtained. Based on the input and output data of the rodless cylinder system, the identification model of the rodless cylinder system is obtained by using the MATLAB system identification toolbox. Finally, with the identification model as the system and the standard input signal as the excitation, the experimental curve and the simulation curve are tracked.

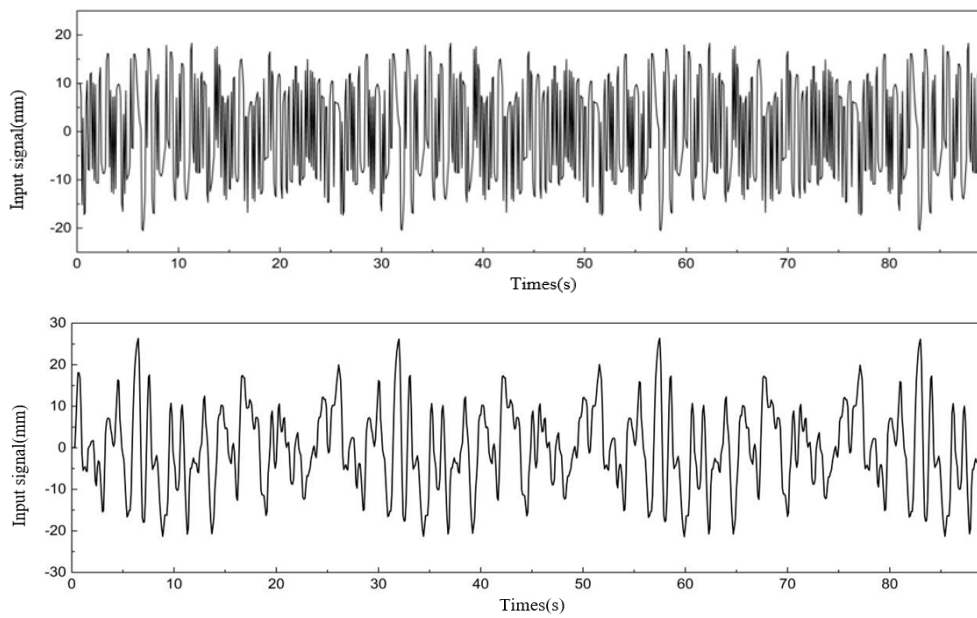


Figure 14 identification of input and output signals

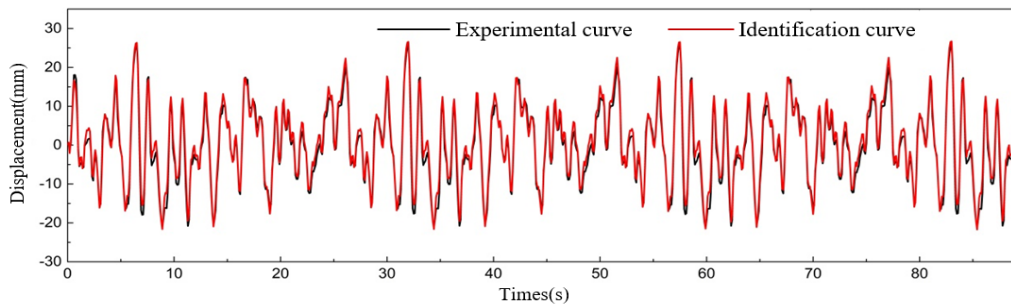


Figure 15 Identification result

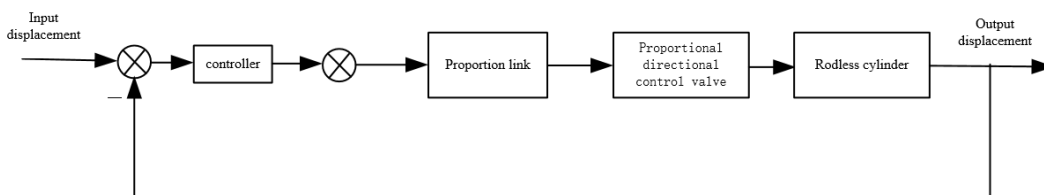
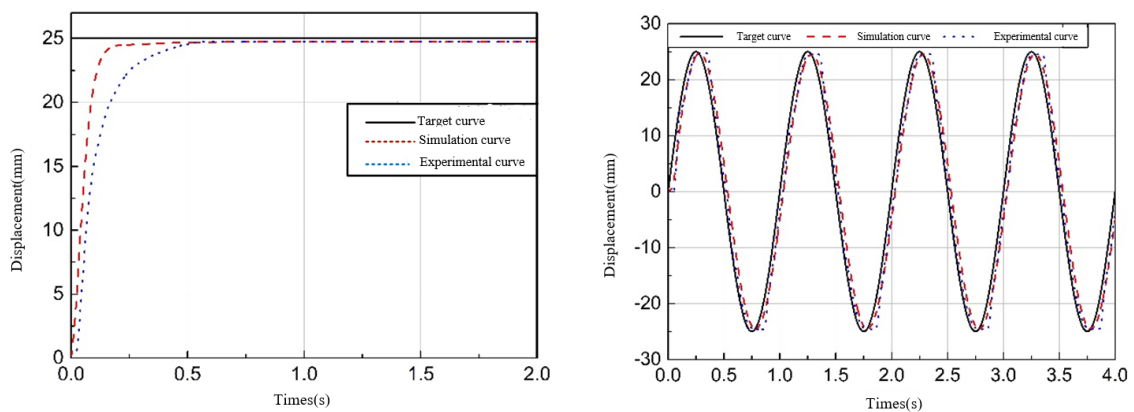


Figure 16 system principle block diagram



(a) Positioning result;

(b) Position tracking result

Figure 17 Comparisons between simulation and experiment

5 Conclusions

Based on the experimental system of position servo control of rodless cylinder, the conclusion is as follows : (1) The friction model of Stribeck mechanical rodless cylinder is established. ($F_s=35.48\text{N}$, $F_c=15.31\text{N}$, $\dot{y}_s=3.27\text{mm/s}$, $\sigma=3.27\text{mm/s}$) ; (2) By establishing the mass flow equation of proportional control valve, mass flow equation and dynamic equation of cylinder, and reducing the influence of friction on the system by friction compensation, the accurate mathematical model of proportional control cylinder system is finally established .(3) The input and output data of valve control cylinder are obtained by experimental test, and the parameters of the system transfer function obtained by MATLAB system box identification to used to verify the correctness of the system model.

Author Contributions: Conceptualization, Yeming ZHANG and Hongwei YUE; Data curation, Kaimin LI; Funding acquisition, Yeming ZHANG; Project administration, Yeming ZHANG; Software, Shuangyang HE and Dongyuan LI; Supervision, Kun LYU and Feng WEI; Writing—original draft, Kaimin LI and Hongwei YUE; Writing—review & editing, Yeming ZHANG and Kaimin LI.

Conflict of Interest: The authors declare no conflict of interest.

Funding: The paper is Supported by Henan Province Science and Technology Key Project (Grant No. 202102210081), the Fundamental Research Funds for Henan Province Colleges and Universities (Grant No. NSFRF140120), Doctor Foundation of Henan Polytechnic University (Grant No.B2012-101).

Acknowledgments: The authors would like to thank Henan Polytechnic University and Beihang University for providing the necessary facilities and machinery to build the prototype of the pneumatic servo system. The authors are sincerely grateful to the reviewers for their valuable review comments, which substantially improved the paper.

References

- [1] SMC (China) Co., Ltd. Modern Practical Pneumatic Technology[M]. Beijing: Machinery Industry Press ,2008.
- [2] Ming Y. Air compressor efficiency in a Vietnamese enterprise [J]. Energy Policy, 2009, 37(6): 2327-2337.
- [3] Zhang Yeming, Cai Maolin. Overall Life Cycle Comprehensive Assessment of Pneumatic and Electric Actuator[J]. Chinese Journal of Mechanical Engineering, 2014, 27(3):584-594.
- [4] Zhang Y, Li K, Wei S, et al. Pneumatic Rotary Actuator Position Servo System Based on ADE-PD Control [J]. Applied Sciences, 2018, 8(3): 406.
- [5] Yeming Zhang, Ke Li, Geng Wang, Maolin Cai. Nonlinear model establishment and experimental verification of a pneumatic rotary actuator position servo system[J]. Energies 2019, 12(6), 1096.
- [6] Yeming Zhang, Hongwei YUE, Ke Li, Maolin Cai. Analysis of power matching on energy saving of pneumatic rotary actuator servo-control system[J]. Chinese Journal of Mechanical Engineering, 2020, 33:30.
- [7] Pedro Luís Andrighetto, Antonio Carlos Valdiero, Leonardo Carlotto. Study of the friction behavior in industrial pneumatic actuators. ABCM Symposium Series in Mechatronics,2006, 2: 369-376.
- [8] Lee E. Schroederl. Experimental Study of Friction in a Pneumatic Actuator at Constant Velocity. Journal of Dynamic Systems, Measurement, and Control, 1993, 9,Vol. 115:575-577.
- [9] Zhang Baihai, Cheng Haifeng, Ma Yanfeng. Experimental study of cylinder friction. Beijing Institute of Technology Journal ,2005,(6):483-487.
- [10] Zhang Baihai, Peng Guangzheng, Liu Qiong, Study on the Influence of Temperature on Friction Characteristics of Cylinder.
- [11] T. Raparelli, A. Manuello, Bertetto and L. Mazza. Experimental and Numerical Study of Friction in an Electrometric Seal for Pneumatic Cylinders. Tribology International. 1997,Volume 30 Number 7: 547-557.
- [12] Belforte. G Raparelli. T, Velardocchia. M. Study of the Behavior of Lip Seals in Pneumatic Actuators.. Lubr. Eng,1993, 45: 775-780.
- [13] Conte M, Manuello A, Mazza L, Visconte C. Measurement of contact pressure in pneumatic actuator seals. In: Proceedings of the AITC-AIT 2006 international conference on tribology,2006.
- [14] G. Belforte, M. Conte, A. Manuello Bertetto, L. Mazza, C. Visconte. Experimental and numerical evaluation of contact pressure in pneumatic seals. Tribology International. 2009,42:169- 175.
- [15] Liu Xiangming, Li Liang. LabVIEW Electro-hydraulic System Identification [J]. Machine and Hydraulic ,2007,35(9):143-145.
- [16] Song Tao, Yu Cungui. Simulation based on MATLAB/Simulink hydraulic servo system identification [J]. Hydraulic and Pneumatic ,2015,(10):120-123.
- [17] Kong Xiangzhen. Dynamic Characteristics and Control of Pneumatic Proportional System [D]. Jinan; Shandong University ,2007.